



This is a repository copy of *Bacterial nanocompartments: structures, functions and applications*.

White Rose Research Online URL for this paper:
<https://eprints.whiterose.ac.uk/179670/>

Version: Accepted Version

Article:

McDowell, H.B. and Hoiczky, E. (2022) Bacterial nanocompartments: structures, functions and applications. *Journal of Bacteriology*, 204 (3). e00346-21. ISSN 0021-9193

<https://doi.org/10.1128/JB.00346-21>

© 2021 American Society for Microbiology. This is an author-produced version of a paper subsequently published in *Journal of Bacteriology*. Uploaded in accordance with the publisher's self-archiving policy.

Reuse

Items deposited in White Rose Research Online are protected by copyright, with all rights reserved unless indicated otherwise. They may be downloaded and/or printed for private study, or other acts as permitted by national copyright laws. The publisher or other rights holders may allow further reproduction and re-use of the full text version. This is indicated by the licence information on the White Rose Research Online record for the item.

Takedown

If you consider content in White Rose Research Online to be in breach of UK law, please notify us by emailing eprints@whiterose.ac.uk including the URL of the record and the reason for the withdrawal request.



eprints@whiterose.ac.uk
<https://eprints.whiterose.ac.uk/>

1 **Bacterial Nanocompartments: Structures, Functions and Applications**

2

3

4

5

Harry Benjamin McDowell and Egbert Hoiczuk

6

7

School of Biosciences, The Krebs Institute, The University of Sheffield,

8

Firth Court, Western Bank, Sheffield, S10 2TN, United Kingdom

9

Phone (+44) 114 222 2733; Fax: (+44) 114 222 2787; Email E.Hoiczuk@Sheffield.ac.uk

10

11

12 **Running Title:** Bacterial nanocompartments

13

14

KEYWORDS Compartmentalization, microcompartment, nanocompartment, encapsulin,

15

gas vesicle, carboxysome, self-assembly, bacterial organelle.

16

McDowell and Hoiczky **Running title:** Bacterial nanocompartments

17 **ABSTRACT**

18 Increasing efficiency is an important driving force behind cellular organization and often
19 achieved through compartmentalization. Long recognized as a core principle of eukaryotic
20 cell organization, its widespread occurrence in prokaryotes has only recently come to light.
21 Despite the early discovery of a few microcompartments such as gas vesicles and
22 carboxysomes, the vast majority of these structures in prokaryotes are less than 100 nm in
23 diameter - too small for conventional light microscopy and electron microscopic thin
24 sectioning. Consequently, these smaller-sized nanocompartments have therefore been
25 discovered serendipitously and then through bioinformatics shown to be broadly distributed.
26 Their small uniform size, robust self-assembly, high stability, excellent biocompatibility, and
27 large cargo capacity make them excellent candidates for biotechnology applications. This
28 review will highlight our current knowledge of nanocompartments, the prospects for
29 applications as well as open question and challenges that need to be addressed to fully
30 understand these important structures.

31

32

McDowell and Hoiczky **Running title:** Bacterial nanocompartments

33 **INTRODUCTION**
34

35 Historically, prokaryotes have long been considered simple, lacking much of the complexity
36 that defines eukaryotic cells. However, discoveries during the last quarter century have
37 challenged this simplified view of bacterial cell biology resulting in two major conceptual
38 revisions. The discovery of FtsZ in the 1990s (1-3) ushered in the age of bacterial
39 cytoskeletal research (reviewed in 4) culminating in the recognition that bacteria, in fact,
40 possess a larger variety of cytoskeletal proteins than eukaryotic cells (5). Likewise, the
41 discovery of ever-increasing numbers of organelle-like structures in bacteria and archaea
42 (Fig. 1) demonstrated that compartmentalization, a key feature of eukaryotic cells is
43 ubiquitously used in prokaryotes. In contrast to bacterial cytoskeletal proteins, the first
44 microcompartment was discovered more than a century ago in aquatic cyanobacteria (6; for
45 a recent review 7). What made the early discovery of gas vesicles possible was their sheer
46 size. Individual structures can have diameters of 120 nm and reach lengths of 1400 nm,
47 making them the only known bacterial compartment visible in a compound light microscope.
48 The advent of transmission electron microscopy in the 1950s led to the discovery of
49 carboxysomes (8). Initially called polyhedral bodies, carboxysomes are 40-200 nm large
50 (quasi)icosahedral protein shells that contain a two-protein enzymatic core formed by
51 carbonic anhydrase and RuBisCO and are essential for carbon fixation (9). Similar
52 microcompartments were later found in *Salmonella* when grown on 1,2-propanediol (10, 11)
53 or ethanolamine (12, 13) and subsequently in a large number of bacterial phyla (14). In
54 contrast to carboxysomes, these metabolosomes are catabolic organelles that detoxify short-
55 chain aldehydes (14, 15). In 2008, serendipity helped discover another type of bacterial
56 compartment, the encapsulins (16). Encapsulins are composed of 20-40 nm wide shells and

McDowell and Hoiczky **Running title:** Bacterial nanocompartments

57 internalized cargo proteins and because their size is smaller than 100 nm they are classified
58 as nanocompartments (17, 18). The first observations of these structures were made in 1994,
59 when high molecular weight protein aggregates were observed in the culture supernatant of
60 *Brevibacterium linens*, noted for their pH stability and bacteriostatic properties (19). It took
61 more than a decade until the nanocompartment nature of these “aggregates” was revealed
62 and the atomic structure of the encapsulin from *Thermotoga maritima* solved using X-ray
63 crystallography (16). Since then, many other encapsulins have been identified and some
64 studied in great detail including encapsulins from *Mycobacterium tuberculosis* (20), *M.*
65 *smegmatis* (21), *Rhodococcus jostii* (22), *Myxococcus xanthus* (18), *Quasibacillus*
66 *thermotolerans* (23), *Synechococcus elongatus* (24), and the archaeon *Pyrococcus furiosus*
67 (25). In fact, increasingly sophisticated comparative genomics has identified encapsulin-
68 encoding genes in at least 31 out of 35 bacterial and 4 out of 5 archaeal phyla (24, 26-28),
69 indicating that these structures are far more widespread than initially thought. Like all
70 bacterial compartments, encapsulins are composed entirely out of protein, no nucleic acid,
71 lipid or carbohydrates have been detected in any of these structures so far, and although
72 encapsulins possess virus-like icosahedral morphologies their phylogenetic relationship to
73 virus capsids is unclear with recent discussions suggesting a possible caudoviral origin (28).
74 What is however clear is that the numerous bacterial compartments strongly support the idea
75 that the principle of cellular compartmentalization predates the origin of eukaryotes and, in
76 fact, appears to be among the first innovations that made primordial cells more efficient (29).
77 Here, we will discuss the recent progress in our understanding of the structure and function
78 of encapsulins as well as ongoing attempts to develop nanotechnological applications for
79 these uniquely versatile structures.

McDowell and Hoiczky **Running title:** Bacterial nanocompartments

80
81 **The structure of encapsulin shells.** Geometrically, encapsulins are icosahedral shells that
82 spontaneously self-assemble from multiple copies of a single protomer that can oligomerize
83 into pentamers and hexamers (16, 25). Topologically, a minimum of twelve pentamers is
84 required, while larger shells can be formed through the addition of variable numbers of
85 hexamers. As a result, encapsulin shells, like virus capsids, are scalable structures that can
86 vary in size (Table 1). To quantitatively characterize this complexity, the triangulation
87 number T is used. Initially introduced to quantitatively describe the geometry of icosahedral
88 viruses (35), T is useful not only to characterize the size of encapsulins but to group them
89 based on their shell architecture. The simplest encapsulins, T=1 icosahedrons are found in *T.*
90 *maritima* and *Mycolicibacterium hassiacum*, where 60 protomers form ca. 24 nm large shells
91 (16, 36). This T=1 geometry is also present in the highly abundant family 2 encapsulins that
92 are found among others in the freshwater cyanobacterium *S. elongatus* and are distinct from
93 all other so far studied encapsulins that are grouped into family 1 (24, 28). The main
94 difference between family 1 and family 2 encapsulins is the lack of an extended N-terminal
95 helix in the latter, instead family 2 encapsulins possess a shorter N-terminal helix with an
96 extended N-terminal arm. However, whether these differences are also present in the cNMP-
97 binding domain-containing family 2 encapsulins remains to be seen. Family 1 encapsulin
98 shells of *Sulfolobus solfataricus*, *P. furiosus* and *M. xanthus* are 32 nm wide T=3
99 icosahedrons that are assembled from 180 protomer subunits (18, 25, 37). Whilst, the
100 encapsulin of *Q. thermotolerans* shows T=4 symmetry, possessing 240 protomer subunits
101 and a diameter of 42 nm (23). This encapsulin possesses the largest atomically resolved shell
102 so far creating an internal cargo space that is 530% larger than that of the T=1 capsids, and

McDowell and Hoiczky **Running title:** Bacterial nanocompartments

103 220% larger than that of the T=3 capsids. Of note, the number of bioinformatically identified
104 possible T=4 encapsulins is so far less than the numbers of T=1 and T=3 shells, which may
105 indicate that among encapsulins like phage capsids larger structures are evolutionary
106 disadvantaged and therefore less common in nature. Two additional less numerous families
107 of encapsulins have been recently identified using computational approaches (28). However,
108 no high-resolution structures exist of any family 3 natural-product-biosynthesis encapsulins
109 or family 4 “truncated A-domain” encapsulins, in which only the compact, five-fold
110 symmetry interface contact-mediating C-terminal A-domain of the HK97-fold is present and
111 all other domains are missing. Thus, it remains to be seen how different their capsids are
112 from solved structures.

113 Notably, the mutual resemblance between encapsulins and icosahedral phage capsids is not
114 only the consequence of their shared geometry but the result of a similar molecular structure
115 of their shell protomer proteins. All encapsulin protomers have the same HK97-like fold as
116 the mature 31 kDa large viral gp5* phage main capsid protein (38), despite a lack of
117 sequence similarity (16, 39). This prominent fold was first observed in the lambdoid Hong
118 Kong 97 (HK97) bacteriophage (39), and has since been found in other tailed phages (40,
119 41), in herpes viruses (42, 43), in the archaeal *Haloarcula sinaiensis* tailed virus 1 (HSTV-
120 1; 44), and in several domains of double stranded DNA viruses (45). Structurally, the HK97-
121 like fold is characterized by the presence of the “spine” α -helix, the peripheral (P-) domain,
122 the axial (A-) domain and the β -hairpin elongated (E-) loop (39) with the E-loop showing
123 the most sequence variability between different protomers (16, 18, 27, 46). While the shell
124 proteins of *P. furiosus* and *M. xanthus* closely match the domain structure of the HK97-fold
125 (18, 25), the *T. maritima* protomer’s homology is limited to the A- and E-loop domains (16).

McDowell and Hoiczky **Running title:** Bacterial nanocompartments

126 The E-loop is essential for the interfacing between subunits, and the relative orientation of it
127 defines the triangulation number and size of the capsid. *T. maritima* encapsulins possess E-
128 loops that are shorter and more rotated than those of larger T=3 capsids. This alteration
129 appears to allow the protomers to form tight β -sheets with their neighbors resulting in the
130 smaller T=1 capsids (16). In contrast, the T=4 encapsulin shells of *Q. thermotolerans* show a
131 non-covalent chain mail topology, a structural feature commonly found in virus capsids.
132 Here, the E-loop and P-domain of each capsid monomer are arranged head to tail, forming
133 interlocking concatemeric rings, which provide the structure with increased level of
134 thermostability (23). This structural motif has also been observed in the T=1 encapsulins of
135 *S. elongatus*, however in this instance, it is an extended N-terminal arm which interlocks
136 with the neighboring subunit to create the chain mail topology (24).

137 Despite their structural similarity, encapsulins and viral capsids differ with respect to a
138 number of important features. To start, encapsulins and capsids use different assembly
139 mechanisms and pathways. Encapsulins self-assemble through the repeated addition of
140 dimers (47), whilst virus capsids make use of more complex assembly processes (48-50). In
141 particular, virus capsid assembly is usually guided by a scaffolding protein that is either N-
142 terminally fused to the protomer (as in HK97) or provided as a separate protein (51). As all
143 studied encapsulins effortlessly self-assemble upon expression in *Escherichia coli*, they do
144 not rely on scaffold-mediated guidance which may be due to their lower T-numbers.
145 Moreover, HK97 capsids undergo large-scale molecular rearrangements of their assembled
146 protomers during capsid maturation (52). These conformational changes are necessary to
147 increase capsid stability and expand cargo capacity. No such protomer movements appear to
148 occur in encapsulins, which may be due to the very different osmotic properties of the

McDowell and Hoiczky **Running title:** Bacterial nanocompartments

149 encapsulated cargos. Although the assembly is different, the resulting structures are
150 remarkably similar potentially suggesting that encapsulins may have evolved from HK97-
151 like phages. Gradually, selection could have erased the integrated phage genome leaving
152 only the gene for the capsid shell, the future encapsulin behind. Whether this scenario is
153 correct is difficult to judge as very rarely genes encoding phage-like proteins are found in
154 today's encapsulin operons (e.g., phage-like replicative helicase in *S. solfataricus*; 37).
155 Nonetheless, the recent lab-based evolutionary conversion of lumazine synthase into an
156 RNA-containing virus-like capsid supports the plausibility of the relatedness of these self-
157 assembling structures (53).

158 Although the rigid encapsulin shells form formidable permeability barriers, they contain
159 multiple pores through which small molecules, ions or organic compounds can enter the
160 encapsulin lumen (22, 54-56). Structurally, these pores are located at the sites of symmetry
161 (3- and 5-fold pores) and at the interface between protomers (2-fold pores) ranging 3-7 Å in
162 size (16, 18, 23, 57). The structures of the two- and five-fold pores appear often to be
163 conserved, whilst the three-fold pores show high levels of variability possibly to
164 accommodate specific substrates (17). Usually, two-fold pores are lined with negatively
165 charged residues, while five-fold pores, like the ones from *T. maritima*, are often uncharged
166 but surrounded by a ring of histidine residues, which may coordinate and help translocate
167 metal ions like iron across the shell (16). Additionally, it has been proposed that the
168 interaction between the shell residues and potential substrates may influence the activity of
169 the encapsulated cargo proteins (16). Compared to *T. maritima*, the encapsulins in *Q.*
170 *thermotolerans* possess 3-fold pores that are larger (7.2 Å) and negatively charged due to the
171 presence of aspartate and glutamate residues, which may facilitate iron uptake (23).

McDowell and Hoiczky **Running title:** Bacterial nanocompartments

172 Remarkably, in this bacterium's encapsulin the two-fold pores appear to be closed. However,
173 the fact that two flexible asparagine side chains are present at the expected site of the pores
174 points to the possibility that the pores may be gated to provide control over substrate
175 permeability (23). Such gating has recently been observed for the 5-fold pores of the
176 *Haliangium ochraceum* encapsulin which can widen from 9 to 24 Å (58).

177 By and large, the size and physicochemical properties of the pores control access to the
178 interior of the encapsulin, permitting small molecules while blocking larger ones. However,
179 the maximum molecular cut-off for access is currently unknown. For example, in *R. jostii*
180 RHA1, the encapsulated dye-decolorizing peroxidase (DyP) degrades nitrated lignin, which
181 is several magnitudes larger than any known pore and it is currently unclear whether and
182 how lignin can actually enter the encapsulin (16, 22, 59). To solve this conundrum, it has
183 been proposed that the encapsulin is either a dynamic structure, able to disassemble upon
184 recognition of the substrate (22) or that the currently unknown pore architecture in this
185 encapsulin is large enough to allow the passage of lignin polymers (see 58). Undoubtedly,
186 pores are essential for encapsulin function allowing cytosolic substrates access to the
187 encapsulated proteins. Thus, pores represent interesting targets for bioengineering to
188 potentially fine-tune substrate access and selectivity (60).

189

190 **Encapsulin cargo proteins.** The initial clue that encapsulins contain cargo proteins came
191 from unaccounted electron densities in X-ray images of the *T. maritima* shell (16).
192 Eventually, eight amino acid residues could be resolved that matched the C-terminal part of a
193 ferritin-like protein encoded in the same operon next to the gene of the encapsulin shell
194 protein. In contrast to its C-terminus, the rest of this ferritin-like protein was too variably

McDowell and Hoiczky **Running title:** Bacterial nanocompartments

195 arranged as to be resolved in the electron density maps. Since then *in-silico* research has
196 shown that many encapsulin cargo proteins possess similar peptide sequences termed
197 targeting or cargo loading peptides (CLP) that specifically target them to the encapsulin.
198 Fortuitously, CLPs are often sufficiently conserved so that they can be used to
199 bioinformatically identify potential cargo proteins (24, 27). By combining this approach with
200 a genome neighbourhood analysis-based strategies thousands of previously unknown
201 potential cargo proteins have recently been identified (28). However, validating cargo
202 proteins and measuring their stoichiometry is more challenging and has e.g. been achieved
203 using STEM measurements of purified natively assembled encapsulins (18). Sequence-wise,
204 CLPs of cargos of family 1 encapsulins are C-terminal peptides (16, 54-56), while CLPs of
205 family 2 and 3 encapsulins are often highly-disordered N- or C-terminal aa sequences (24,
206 28). Like in *T. maritima*, cargo proteins are usually expressed in co-regulated operons with
207 their corresponding shell protein and it is generally assumed that they are loaded co-
208 translationally although experimental evidence for this packaging mode is currently lacking
209 (16, 27). However, there are exceptions to this rule. In *P. furiosus*, the cargo gene is fused
210 with that of the shell protein and they are expressed as a single polypeptide (25). Other
211 bacteria possess additional cargo proteins and these ‘secondary cargos’ are not encoded in
212 the encapsulin operon (18, 61). The alternate genetic loci of these secondary cargos
213 challenge a simple co-translationally packaging model during assembly (54, 55). How the
214 cells solve this problem is currently unclear.

215 Research has shown that CLPs are both necessary and sufficient for the encapsulation of
216 cargo proteins (16, 27, 54-56, 61, 62). The deletion of the CLP from the C-terminus of DyP,
217 a cargo protein in *T. maritima*, prevented encapsulation (16). While in *R. erythropolis* N771,

McDowell and Hoiczky **Running title:** Bacterial nanocompartments

218 the addition of CLPs to non-native cargos such as enhanced green fluorescent protein
219 (eGFP) and luciferase facilitated efficient packaging (54). This flexibility of packaging is
220 one of the key features that make encapsulins attractive for bioengineering.
221 As space is limited inside encapsulins, cargo protein loading is restricted raising questions of
222 how many cargo proteins can fit into a single shell and how they are organized. In theory,
223 each capsid protomer has one CLP binding site and therefore could bind one cargo protein
224 but in practice the number of cargo proteins must be lower than that of protomers. Steric
225 hindrance among the cargo proteins, the need for proper folding and shell closure all
226 constrain cargo encapsulation (16, 47). For example, it has been shown that DyP
227 oligomerizes into hexameric rings upon encapsulation in *B. linens*, with one hexamer being
228 assembled in each shell (47). In the same shell, twelve molecules of GFP can be loaded
229 weighing 400 kDa compared to the 240 kDa of the DyP hexamer. Thus, the spatial
230 arrangement of the molecules is more important than the size when determining packaging
231 into encapsulins. Ferritin-like proteins have been shown to oligomerize into decamers during
232 packing, with each decamer being significantly smaller than a DyP hexamer (56). This
233 difference in size means 120 ferritin-like proteins fit within a T=1 shell compared with the 6
234 DyPs, thus drastically increasing the cargo to shell ratio (47). Cargo loading is further
235 complicated in multi-cargo encapsulins. As described, *M. tuberculosis* and *M. xanthus* need
236 to package three or four different cargo proteins, respectively thereby increasing the risk for
237 steric clashes (18, 61, 63). Perhaps, these bacteria use currently unknown mechanisms for
238 regulating packaging of heterologous cargos, as a high level of selectivity for cargo is
239 maintained as the complexity of cargo increases (18, 47, 55). Maybe cargo protein
240 oligomerization plays a not yet understood role in the control of cargo packaging. Another

McDowell and Hoiczky **Running title:** Bacterial nanocompartments

241 option, found in iron-mineralizing encapsulin-associated Firmicutes (IMEF) could be the use
242 of both N- and C-terminal CLPs on different cargo proteins, which may provide higher
243 levels of control over packaging (27). Whereas it is thought that the relative concentrations
244 of the substrates in proximity to the binding site is used to control the loading in other
245 systems. Additionally, there may exist transcriptional control systems that limit the relative
246 production of each cargo protein, allowing for increased packaging efficiency. One way to
247 address these issues would be *in situ* cryo-electron microscopy of the cargo complexes.
248 Although data exist that indicate sub-stoichiometric occupancy of binding sites (21), the
249 resolution in many tomograms is not yet high enough to definitively answer these questions
250 (18, 58).

251

252 **Biological functions of encapsulins.** Although the biochemical properties of the cargo
253 proteins are key to unravelling the biological functions of encapsulins, answers are not
254 always straightforward. To start, most bacteria produce un-encapsulated versions of their
255 cargo proteins (16, 27). In addition, functional assignments are often complicated by the lack
256 of physiological data for the mostly bioinformatically identified encapsulin systems (28)
257 and, finally, the observation of assembled encapsulins in culture supernatants have raised
258 questions about the localisation of these structures (19).

259 Despite these challenges recent research has started to provide crucial information.
260 Importantly, packaging of fragile proteins into stable shell structures may increase the life
261 time of the cargo, as encapsulin shells have increased thermo- and pH-stability (16, 19, 22),
262 as well as providing protection from proteases (54, 55). In fact, the prevalence of encapsulins
263 in extremophiles suggests that cargo packaging may be particularly beneficial under harsh

McDowell and Hoiczky **Running title:** Bacterial nanocompartments

264 conditions (27). Interestingly, atomic force microscopy has shown that cargo-binding
265 decreases the shell's mechanical stiffness due to conformational changes of the shell
266 structure, which may have implications for the overall stability of encapsulins (47, 64).

267 Surprisingly, despite their intracellular assembly, it is not completely clear whether
268 encapsulins are intra- and/or extracellular structures. Their initial discovery in culture
269 supernatants pointed to possible extracellular functions (16, 18, 19, 22), however currently
270 available evidence suggests that they are cytosolic and appear only in the supernatant after
271 cell lysis because of their resistance to degradation (17). This hypothesis is also supported by
272 the lack of any known bacterial transport system capable of translocating an assembled
273 structure of this size (26, 65). However, this does not rule out that encapsulin-producing cells
274 may undergo coordinated lysis to release large numbers of these structures to either control
275 physicochemical parameters of the medium, degrade substances, poison other cells or
276 provide metabolites for their kin.

277 Based on large-scale bioinformatics analyses of their potential cargos, encapsulins have been
278 suggested to play roles in a wide range of physiological responses including stress
279 resistance, toxin sequestration, natural product biosynthesis, catabolic and anabolic
280 metabolism and anaerobic hydrogen production (26, 28). However, the validity of these
281 assigned functions and the precise role of the encapsulin shell in these different processes
282 has been studied in only a handful of instances.

283 One well studied function is their role in oxidative stress response, protecting the cell from
284 peroxide-related damage. DyP cargo enzymes such as those found in *M. tuberculosis* are
285 active against polyphenolic compounds such as azo dyes, although their natural substrates
286 are unknown (56, 59, 61, 66). *In vitro* studies have shown that the peroxidase activity of DyP

McDowell and Hoiczky **Running title:** Bacterial nanocompartments

287 increases 8-fold upon encapsulation, perhaps due to the increased protection provided by the
288 shell or by increasing the local substrate concentration akin to the accumulation of CO₂ in
289 carboxysomes (67-70). The deletion of the shell protein, EncA, from *M. xanthus* resulted in a
290 strain that was more sensitive to hydrogen peroxide than the wild type (18). Increased
291 peroxide sensitivity has also been observed when the ferritin-like cargo protein is deleted
292 from the *M. tuberculosis* system (71). Importantly, all other cargo proteins in *M. tuberculosis*
293 appear to contribute to the overall oxidative stress resistance of the bacterium (61). In
294 contrast, the DyP-containing encapsulin of *R. jostii* RHA1 has been implicated in a catabolic
295 reaction. Deleting the *dypB* gene, results in a mutant which generated encapsulins that were
296 unable to break down the substrate nitrated lignin (22).

297 Probably, the best studied function of encapsulins is the mineralization and storage of iron.
298 Iron is essential for many cellular processes but in excess can cause oxidative damage. If
299 iron homeostasis is not maintained, Fe(II) is oxidized to insoluble Fe(III) and reactive
300 oxygen species like free hydroxyl radicals are formed *via* the Fenton reaction that can damage
301 cellular structures (72-74). Hence, it is hypothesised that iron-sequestering encapsulins
302 constitute a back-up iron management system, alongside the traditional ferritin system, that
303 becomes active during times of stress. For example, amino acid starvation of *M. xanthus* up-
304 regulates the number of encapsulins fivefold (from 4-5 to 20-25 per cell) with each structure
305 capable of storing ~30,000 iron atoms that form 5-6 nm granules within the organelle's
306 20 nm wide core (18). The observation that the more stress-resistant tan variants of this
307 bacterium appear to not contain any assembled encapsulin during growth and, upon
308 starvation, form only 4-5 particles per cell, the same number found in the more sensitive
309 yellow strain during vegetative growth, highlights the fact that encapsulin assembly is not

McDowell and Hoiczky **Running title:** Bacterial nanocompartments

310 only dependent on environmental conditions but also controlled by strain-specific factors
311 (unpublished results and 75). In contrast to *M. xanthus*, *Q. thermotolerans* lacks traditional
312 ‘ferritins’ and therefore appears to use encapsulins as their primary system for iron
313 homeostasis (23). As the larger size means that each *Q. thermotolerans* encapsulin can store
314 up to ~83,000 iron atoms (23). Interestingly, it appears that all encapsulin proteins are
315 necessary for efficient iron storage. Research using *Bacillaceae bacterium* MTCC 10057
316 encapsulin expressed in *E. coli* determined that only when the shell and both cargo proteins
317 were expressed was iron mineralized efficiently *in vivo*, despite one of the cargo proteins,
318 Fer, not being essential for iron mineralization (23). Furthermore, *E. coli* only showed
319 increased resistance to hydrogen peroxide when the iron content of the medium was
320 increased, indicating that iron storage and oxidative stress response are linked (27). Another
321 type of cargo protein linked to oxidative stress are hemerytherins (27). These metalloproteins
322 are capable of reversibly binding O₂ through an iron atom bound by an oxo bridge (75). In
323 encapsulins, they are found exclusively in T=1 capsids organised into 20 sets of dimers (63,
324 77, 78). Expression of the hemerythrin-encapsulin system from *Streptomyces sp.* AA4 in *E.*
325 *coli* showed that for optimal levels of protection both, the shell and cargo were necessary
326 (27).
327 Encapsulins have also been identified as metabolically important in anaerobic ammonium
328 oxidising (anammox) bacteria (27). Anammox bacteria oxidise ammonium with nitrite
329 creating dinitrogen gas as part of their metabolism (79, 80). Using growth curve assays, it
330 has been shown that encapsulins aid anammox bacteria in resisting hydroxylamine-related
331 stress (27, 81, 82) by sequestering the toxic intermediate hydrazine (80, 83), through a nitrite
332 reductase-like (NiR)/hydroxylamine oxidoreductase (HAO)-like fusion cargo protein (82,

McDowell and Hoiczky **Running title:** Bacterial nanocompartments

333 83). The NiR-like cargo has been hypothesised to be a laccase, a multicopper enzyme which
334 oxidises aromatics using oxygen (81). Intriguingly, anammox encapsulins could also
335 function extracellularly, as their NIR-like cargo can help maintain an anaerobic environment,
336 a prerequisite for the bacterium's survival (81). However, due to the difficulties of working
337 with anaerobes and the lack of genetic tools no work has so far been done exploring this
338 possibility.

339

340 **Biotechnological applications of nanocompartments.** Using biological structures to solve
341 medical and engineering problems has long been a goal of nanotechnology. Thus far, various
342 biological nanostructures have been explored including micelles (84), liposomes (85),
343 polymer nanoparticles (86), virus-like particles (87), DNA origami structures (88), and many
344 different protein-based cages (89, 90). Despite being functional, these nanostructures lack
345 the ability to self-assemble *in vivo*, which is one of the great advantages of encapsulins.
346 Although exceptionally well suited, encapsulins have, however, limitations that remain to be
347 addressed. One such limitation is their small pore size of 3-4 Å, which is ideal for the
348 transfer of ions or small substrates, but severely limits access of larger molecules (16, 36,
349 57). Encouragingly, site directed mutagenesis of the pore-forming loop region of the *T.*
350 *maritima* shell protein has recently tripled the pore size to ~11 Å. This modification resulted
351 in a 7-fold increase in the rate of diffusion across the pores (57). Hence, additional
352 modifications could further improve diffusion and the recent discovery of naturally
353 occurring larger pores (5-9 and 24 Å) in the encapsulins of *M. hassiacum* (36) and of *H.*
354 *ochraceum* (58) respectively indicates that this goal may be achievable with smaller
355 alterations. Another area for research is cargo packaging. While the well-defined CLP tags

McDowell and Hoiczky **Running title:** Bacterial nanocompartments

356 have been successfully used to package a wide range of heterologous cargo proteins (54, 55,
357 91), inorganic molecules like gold nanoparticles have only recently been explored as cargos
358 (92). Moreover, recent systematic investigations of the CLP-shell interaction (93), shell
359 stabilization and purification strategies (94, 95), and the design of an on-demand reversible
360 assembling encapsulin (96) may increase control over the assembly process. Despite this
361 overall progress, there are a number of open questions: How do the disordered packaging
362 signals work and can they be used akin CLPs? What is the best strategy to package multi-
363 protein complexes? How are these complexes organised inside the protein cage and how
364 does this impact functionality (97)? Can the procedures for T=1 capsids simply be scaled up
365 for the larger T=3 and T=4 shells? And finally, are there restrictions to the hosts in which
366 encapsulins can be introduced? While prokaryotic hosts appear to be generally permissive
367 (27, 56), few eukaryotic hosts such as yeast, mice and select mammalian and insect cell lines
368 have so far been tested for the production of encapsulins (98-100). To highlight the
369 nanotechnological potential of encapsulins, we will in the following briefly discuss four of
370 the many theoretically possible applications (Fig. 2) that are currently moving from concept
371 to commercialization:

372
373 **Vaccines.** For more than 40 years live or recombinant derivative adenovirus vaccines have
374 been used for immunization (101, 102). So, it's no wonder that the virus-like nature of
375 encapsulins has attracted attention as vaccine platform. In particular, their ability to package
376 immunogenic cargos offers a second, very different mode of antigen presentation besides the
377 surface display of adenovirus vaccines. The potential of both modes of presentation to
378 induce an immune response has been shown through the production of a novel influenza A
379 vaccine (103). For this vaccine, the *T. maritima* encapsulin was functionalized to display the

McDowell and Hoiczky **Running title:** Bacterial nanocompartments

380 matrix protein 2 ectodomain, an immunologically important epitope from influenza A on its
381 surface whilst encapsulating GFP as a reporter. Following assembly, studies in mice showed
382 specific antibody production against both the surface-displayed epitope and the GFP cargo
383 (104). Likewise, encapsulin surface-associated OT-1 antigen has been used to activate CD8+
384 T cells for tumour rejection. Upon uptake of the OT-1-presenting encapsulins by
385 phagosomes, corresponding antigen-specific T-cells were produced that significantly
386 suppressed a B16-OVA melanoma (105). Consequently, encapsulin could become valuable
387 alternatives to currently existing vaccines, while their lack of nucleic acid could increase
388 vaccine acceptance.

389

390 **Drug Delivery.** Encapsulation of drug molecules increases efficiency of drug delivery and
391 reduces the risk of side effects (106, 107). To explore encapsulins as drug delivery vehicles,
392 *T. maritima* encapsulins displaying the hepatocellular carcinoma cell-binding peptide SP94
393 were chemically coupled to the anticancer prodrug doxorubicin. Efficacy wise the coupled
394 prodrug showed the same killing efficiency as the free prodrug molecule, while the
395 combination of a targeting ligand and therapeutic allowed site-selective delivery to HepG2
396 carcinoma cells (46, 108). Moreover, use of fluorescently labelled encapsulins of *T. maritima*
397 (109) and *B. linens* (110) allowed images to be taken of interactions with their target cell
398 populations highlighting their stability during the uptake process. More recently, PEGylation
399 has been used to further improve the usability of encapsulins as drug carriers (111).
400 PEGylation is a widely-accepted drug carrier modification, that increases the drug delivery
401 efficiency by decreasing the visibility of the carrier to phagocytes and by preventing carrier
402 aggregation. For example, using surface-exposed lysine residues, the encapsulins of *R.*

McDowell and Hoiczky **Running title:** Bacterial nanocompartments

403 *erythropolis* N771 were successfully PEGylated and encouragingly, the modification did not
404 interfere with the assembly and disassembly of the structure (111). However, inspection
405 revealed that the shells were empty, meaning that simultaneous cargo loading and
406 PEGylation may destabilize encapsulin even more than cargo loading does alone (47).
407 Nonetheless, successful PEGylation is likely achievable and would greatly improve drug
408 delivery.

409

410 **Biocatalysts.** Encapsulins are essentially biocatalysts that accelerate the kinetics of
411 biochemical reactions through an increase in substrate concentration within a confined space
412 (112). Given their theoretical promiscuity, any encapsulated protein should in practice be
413 able to catalyse the corresponding reaction. In a proof of principle study, five different
414 enzymes, a catalase, a monooxygenase, two oxidases and a peroxidase were successfully
415 packaged in the encapsulin of *M. hassiacum* (36). Four of the five enzymes were
416 enzymatically active, while the fifth protein, the flavin-containing monooxygenase was
417 inactive likely due to the 9 Å pores blocking access of the cofactor NADPH, again
418 highlighting the importance of pore size (57). Additionally, encapsulins have been used as
419 nanofactories for e.g. the production of silver nanoparticles and antimicrobial peptides.
420 Modifications to the *T. maritima* encapsulins yielded monodisperse silver nanoparticles that
421 possessed better antimicrobial activity than chemically manufactured ones (113). Another
422 functional nanoparticle resulted from the fusion of the antimicrobial peptide HBCM2 to the
423 N-terminus of the *T. maritima* shell protein. The recombinant purified particles showed
424 antibacterial activity against *E. coli* as a result of their surface-exposed antimicrobial
425 peptides (114). In essence however, all these examples are so far mostly very basic attempts
426 to harness the biocatalytic capacity of encapsulins (115). Next generation T=3 and T=4

McDowell and Hoiczky **Running title:** Bacterial nanocompartments

427 designer encapsulins should allow larger multi-protein cargos and the potential to perform
428 highly complex metabolic reactions.

429

430 **Imaging probes.** Encapsulins' ability to sequester or to display light and electron
431 microscopic imageable substances make them ideal imaging probes. A quality that is further
432 enhanced by their robust stability, small size and ease of tissue penetration (109). In its
433 simplest form, CLP-carrying GFP is used as cargo and visualized using fluorescent
434 microscopy. However, photo instability and the low number of GFP molecules per capsid
435 limit this method. Recently, surface-bound spiropyran fluorophores have been used to boost
436 fluorescence (116). As each *B. linens* shell monomer possesses four surface-accessible
437 lysines, a total of 240 fluorophores can be coupled to a single encapsulin. Experiments
438 showed that the spiropyran was stable through at least five cycles of photo-isomerization
439 creating a photo-switchable probe (117). To further improve this approach, dual
440 functionalization of the shell surface has been introduced using the SpyCatcher system that
441 allows combining fluorescent proteins and targeting peptides thereby creating targetable
442 imaging probes (118). Importantly, these highly fluorescent probes can be used for single
443 molecule imaging *in vivo* and could improve resolution in STORM and PALM microscopy.
444 Finally, iron sequestering nanocompartments have been used as a probe for MRI scans (98).
445 Normally, metalloproteins, ferritins or tyrosine are used as reporters during MRI because of
446 their paramagnetic properties (119). However, iron-sequestering encapsulins produce
447 paramagnetic particles large enough to be visualised during MRI (98) and can also be used
448 for magnetic hyperthermia therapy (120). Excitingly, the high iron content of these

McDowell and Hoiczky **Running title:** Bacterial nanocompartments

449 encapsulins also allows their use as multiplex imaging probes in electron microscopy
450 addressing a long-standing imaging need (99).

451

452 **Outlook.** Since their serendipitous discovery in 2008, encapsulin research has made
453 remarkable progress. Cryo-electron microscopy has revealed the virus-like HK97-fold of
454 their shells, while increasingly sophisticated bioinformatics has discovered that encapsulins
455 of this fold type are found in almost all bacterial and archaeal phyla. Nonetheless there are
456 many unanswered questions. Are HK97-fold encapsulins the only type of encapsulins or are
457 their other structural archetypes awaiting to be discovered? What determines the size of
458 encapsulins and how large can they get? Given the narrow range of sizes, do evolutionary
459 constraints, like in viruses, favour certain sizes over others? And speaking of viruses what is
460 the precise evolutionary relationship between these two structures? Are encapsulins,
461 prokaryotic proteins turned viruses turned encapsulins or is their relationship more tangled?
462 Another poorly understood aspect is the dynamics of encapsulins. How precisely do they
463 assemble - in one step or from the inside out and once assembled can they spontaneously
464 disassemble or do they need auxiliary molecules? Other unresolved questions relate to their
465 functions. While bioinformatics has greatly helped identify potential functions through cargo
466 proteins, experiments are needed to confirm them. This is particularly relevant for cargos
467 with disordered targeting signals that are not encoded in core operons. Another important
468 question is whether these extremely durable structures perform some of their functions
469 extracellularly e.g. by manipulating the microbe's environment, producing signals,
470 delivering toxins or simply providing metabolites for its kin? While the answers to these
471 questions will undoubtedly inform our fundamental understanding, bioengineering will

McDowell and Hoiczky **Running title:** Bacterial nanocompartments

472 likely focus on more tangible aspects such as the recombinant large scale production of
473 encapsulins, the packaging of novel cargos, the control of the pore size, shell stability and
474 cargo capacity. Other relevant aspects are the functionalization of the capsid shell through
475 ligands, probes, targeting molecules etc. Although currently mostly conceptual, these studies
476 will become more and more applied as we begin to better understand these small but highly
477 versatile structures.

478

479 **ACKNOWLEDGMENTS**

480 We would like to thank Alasdair Steven and Dennis Winkler (NIH) for sharing their
481 knowledge and enthusiasm for the HK97-fold and their continuing support and Thomas
482 Walther (University of Sheffield) and members of the Hoiczky lab for stimulating
483 discussions and advice. This work was supported by a University of Sheffield EPSRC
484 Doctoral Training Partnership (DTP) Scholarship to HBM (EP/T517835/1). The authors
485 declare that no potential conflict of interests exists.

486

McDowell and Hoiczky **Running title:** Bacterial nanocompartments

487 **REFERENCES**

488

489 1. RayChaudhuri D, Park JT. 1992. *Escherichia coli* cell-division gene *ftsZ* encodes a
490 novel GTP-binding protein. *Nature* **359**:251-254.

491

492 2. De Boer P, Crossley R, Rothfield R. 1992. The essential bacterial cell division protein
493 FtsZ is a GTPase. *Nature* **359**:254-256.

494

495 3. Mukherjee A, Dai K, Lutkenhaus J. 1993. *Escherichia coli* cell division protein FtsZ is a
496 guanine nucleotide binding protein. *Proc Natl Acad Sci USA* **90**:1053-1057.

497

498 4. Erickson HP. 2007. Evolution of the cytoskeleton. *BioEssays* **29**:668-677.

499

500 5. Wagstaff J, Löwe J. 2018. Prokaryotic cytoskeletons: protein filaments organizing small
501 cells. *Nat Rev Microbiol* **16**:187-201.

502

503 6. Klebahn H. 1895. Gasvakuolen, ein Bestandteil der Zellen der wasserblütebildenden
504 Phycochromaceen. *Flora (Jena)* **80**:241-283.

505

506 7. Pfeifer F. 2012. Distribution, formation and regulation of gas vesicles. *Nat Rev*
507 *Microbiol* **10**:705-715.

508

509 8. Drews G, Niklowitz W. 1956. Beiträge zur Cytologie der Blaualgen. II. Zentroplasma

McDowell and Hoiczky **Running title:** Bacterial nanocompartments

- 510 und granuläre Einschlüsse von *Phormidium uncinatum*. *Arch Mikrobiol* **24**:147-162.
511
- 512 9. Shively JM, Ball F, Brown DH, Saunders RE. 1973. Functional organelles in
513 prokaryotes: polyhedral inclusions (carboxysomes) of *Thiobacillus neapolitanus*.
514 *Science* **182**:584-586.
515
- 516 10. Bobik TA, Havemann GD, Busch RJ, Williams DS, Aldrich HC. 1999. The propanediol
517 utilization (pdu) operon of *Salmonella enterica* serovar typhimurium LT2 includes genes
518 necessary for formation of polyhedral organelles involved in coenzyme B₁₂-dependent
519 1,2- propanediol degradation. *J Bacteriol* **181**:5967-5975.
520
- 521 11. Havemann GD, Sampson EM, Bobik TA. 2002. PduA is a shell protein of polyhedral
522 organelles involved in coenzyme B₁₂-dependent degradation of 1,2-propanediol in
523 *Salmonella enterica* serovar typhimurium LT2. *J Bacteriol* **184**:1253-1261.
524
- 525 12. Kofoid E, Rappleye C, Stojiljkovic I, Roth J. 1999. The 19-gene ethanolamine (eut)
526 operon of *Salmonella typhimurium* encodes five homologues of carboxysomes shell
527 proteins. *J Bacteriol* **181**:5317-5329.
528
- 529 13. Pokhrel A, Kang S, Schmidt-Dannert. 2021. Ethanolamine bacterial
530 microcompartments: from structure, function studies to bioengineering applications.
531 *Curr Opin Microbiol* **62**:28-37.
532

McDowell and Hoiczky **Running title:** Bacterial nanocompartments

- 533 14. Axen SD, Erbilgin O, Kerfeld CA. 2014. A taxonomy of bacterial microcompartment
534 loci constructed by a novel scoring method. *PLoS Comput Biol* **10**:e1003898.
535
- 536 15. Kerfeld CA, Erbilgin O. 2015. Bacterial microcompartments and the modular
537 construction of microbial metabolism. *Trends Microbiol* **23**:22-34.
538
- 539 16. Sutter M, Boehringer D, Gutmann S, Günther S, Prangishvili D, Loessner MJ, Stetter
540 KO, Weber-Ban E, Ban N. 2008. Structural basis of enzyme encapsulation into a
541 bacterial nanocompartment. *Nat Struct Biol* **15**:939-947.
542
- 543 17. Nichols RJ, Cassidy-Amstutz C, Chaijarasphong T, Savage DF. 2017. Encapsulins:
544 molecular biology of the shell. *Crit Rev Biochem Mol* **52**:583-594.
545
- 546 18. McHugh CA, Fontana J, Nemecek D, Cheng N, Aksyuk AA, Heymann JB, Winkler DC,
547 Lam AS, Wall JS, Steven AC, Hoiczky E. 2014. A virus-like nanocompartment that
548 stores iron and protects bacteria from oxidative stress. *EMBO J* **33**:1896-1911.
549
- 550 19. Valdes-Stauber N, Scherer S. 1994. Isolation and characterization of linocin M18, a
551 bacteriocin produced by *Brevibacterium linens*. *Appl Environ Microbiol* **60**:3809-3814.
552
- 553 20. Rosenkrands I, Rasmussen PB, Carnio M, Jacobsen S, Theisen M, Andersen P. 1998.
554 Identification and characterization of a 29-kilodalton protein from *Mycobacterium*
555 *tuberculosis* culture filtrate recognized by mouse memory effector cells. *Infect Immun*

McDowell and Hoiczky **Running title:** Bacterial nanocompartments

556 **66:2728-2735.**

557

558 21. Tang Y, Mu A, Zhang Y, Zhou S, Wang W, Lai Y, Zhou X, Liu F, Yang X, Gong H,
559 Wang Q, Rao Z. 2021. Cryo-EM structure of *Mycobacterium smegmatis* Dyp-loaded
560 encapsulin. *Proc Natl Acad Sci USA* **118**:e2025658118.

561

562 22. Rahmanpour R, Bugg TDH. 2013. Assembly *in vitro* of *Rhodococcus jostii* RHA1
563 encapsulin and peroxidase DypB to form a nanocompartment. *FEBS J* **280**:2097-2104.

564

565 23. Giessen TW, Orlando BJ, Verdegaal AA, Chambers MG, Gardener J, Bell DC, Birrane
566 G, Liao M, Silver PA. 2019. Large protein organelles form a new iron sequestration
567 system with high storage capacity. *eLife* **8**:e46070.

568

569 24. Nichols RJ, LaFrance B, Phillips NR, Oltrogge LM, Valentin-Alvarado LE, Bischoff AJ,
570 Nogales E, Savage DF. 2021. Discovery and characterization of a novel family of
571 prokaryotic nanocompartments involved in sulfur metabolism. *eLife* **10**:e59288.

572

573 25. Akita F, Chong KT, Tanaka H, Yamashita E, Miyazaki N, Nakaishi Y, Suzuki M,
574 Namba K, Ono Y, Tsukihara T, Nakagawa A. 2007. The crystal structure of a virus-like
575 particle from the hyperthermophilic archaeon *Pyrococcus furiosus* provides insight into
576 the evolution of viruses. *J Mol Biol* **368**:1469-1483.

577

578 26. Radford D. 2015. Understanding the encapsulins: prediction and characterization of

McDowell and Hoiczky **Running title:** Bacterial nanocompartments

- 579 phage capsid-like nanocompartments in prokaryotes. PhD thesis, University of Toronto.
580 Available from <http://tspace.library.utoronto.ca/handle/1807/69450> [accessed September
581 2021].
582
583 27. Giessen TW, Silver PA. 2017. Widespread distribution of encapsulin nanocompartments
584 reveal functional diversity. *Nature Microbiol* **2**:17029.
585
586 28. Andreas MP, Giessen TW. 2021. Large-scale computational discovery and analysis of
587 virus-derived microbial nanocompartments. *Nat Commun* **12**:4748.
588
589 29. Koonin EV, Martin W. 2005. On the origin of genomes and cells within inorganic
590 compartments. *Trends Genet* **21**:647-654.
591
592 30. Ladenstein R, Ritsert K, Huber R, Richter G, Bacher A. 1994. The lumazine
593 synthase/riboflavin synthase complex of *Bacillus subtilis*. *Eur J Biochem* **223**:1007-
594 1017.
595
596 31. Abrescia NGA, Bamford DH, Grimes JM, Stuart DI. 2012. Structure unifies the viral
597 universe. *Annu Rev Biochem* **81**:795-822.
598
599 32. Walsby AE. 1994. Gas vesicles. *Microbiol Rev.* **58**:94-144.
600
601 33. Cai F, Dou Z, Bernstein S, Leverenz R, Williams E, Heinhorst S, Shively J, Cannon G,

McDowell and Hoiczky **Running title:** Bacterial nanocompartments

- 602 Kerfeld C. 2015. Advances in understanding carboxysome assembly in *Prochlorococcus*
603 and *Synechococcus* implicate CsoS2 as a critical component. *Life* **5**:1141-1171.
604
- 605 34. Parsons J, Dinesh S, Deery E, Leech H, Brindley A, Heldt D, Frank S, Smales C,
606 Lünsdorf H, Rambach A, Gass M, Bleloch A, McClean K, Munro A, Rigby S, Warren
607 M, Prentice M. 2008. Biochemical and structural insights into bacterial organelle form
608 and biogenesis. *J Biol Chem* **283**:14366-14375.
609
- 610 35. Casper DLD, Klug A. 1962. Physical principles in the construction of regular viruses.
611 *Cold Spring Harb Symp Quant Biol* **27**:1-24.
612
- 613 36. Lončar N, Rozeboom HJ, Farnken LE, Stuart MCA, Fraaije MW. 2020. Structure of a
614 robust bacterial protein cage and its application as a versatile biocatalytic platform
615 through enzyme encapsulation. *Biochem Biophys Res Commun* **529**:548-553.
616
- 617 37. Heinemann J, Maaty WS, Gauss GH, Akkaladevi N, Brumfield SK, Rayaprolu V,
618 Young MJ, Lawrence CM, Bothner B. 2011. Fossil record of an archaeal HK97-like
619 provirus. *Virology* **417**: 362-368.
620
- 621 38. Duda RL, Hempel J, Michel H, Shabanowitz J, Hunt D, Hendrix RW. 1995. Structural
622 transitions during bacteriophage HK97 head assembly. *J Mol Biol* **247**:618-635.
623
- 624 39. Wikoff WR, Liljas L, Duda RL, Tsuruta H, Hendrix RW, Johnson JE. 2000.

McDowell and Hoiczky **Running title:** Bacterial nanocompartments

- 625 Topologically linked protein rings in the bacteriophage HK97 capsid. *Science* **289**:2129-
626 2133.
- 627
- 628 40. Fokine A, Leiman PG, Shneider MM, Ahvazi B, Boeshans KM, Steven AC, Black LW,
629 Mesyanzhinov VV, Rossmann MG. 2005. Structural and functional similarities between
630 the capsid proteins of bacteriophages T4 and HK97 point to a common ancestry. *Proc*
631 *Natl Acad Sci USA* **102**:7163-7168.
- 632
- 633 41. Agirrezabala X, Velázquez-Muriel JA, Gómez-Puertas P, Scheres SHW, Carazo JM,
634 Carrascosa JL. 2007. Quasi-atomic model of bacteriophage T7 procapsid shell: insights
635 into the structure and evolution of a basic fold. *Structure* **15**:461-472.
- 636
- 637 42. Baker ML, Jiang W, Rixon FJ, Chiu W. 2005. Common ancestry of herpesviruses and
638 tailed DNA bacteriophages. *J Virol* **79**:14967-14970.
- 639
- 640 43. Cardone G, Heymann JB, Cheng N, Trus BL, Steven AC. 2012. Procapsid assembly,
641 maturation, nuclear exit: dynamic steps in the production of infectious herpesvirions.
642 *Adv Exp Med Biol* **726**:423-439.
- 643
- 644 44. Pietilä MK, Laurinmäki P, Russell DA, Ko CC, Jacobs-Sera D, Hendrix RW, Bamford
645 DH, Butcher SJ. 2013. Structure of the archaeal head-tailed virus HSTV-1 completes the
646 HK97 fold story. *Proc Natl Acad Sci USA* **110**:10604-10609.
- 647

McDowell and Hoiczky **Running title:** Bacterial nanocompartments

- 648 45. Koonin EV, Dolja VV, Krupovic M, Varsani A, Wolf YI, Yutin N, Zerbini FM, Kuhn
649 JH. 2020. Global organization and proposed megataxonomy of the virus world.
650 *Microbiol Mol Biol Rev* **84**:e00061-19.
651
- 652 46. Moon H, Lee J, Min J, Kang S. 2014. Developing genetically engineered encapsulin
653 protein cage nanoparticles as a targeted delivery nanoplatform. *Biomacromolecules*
654 **15**:3794-3801.
655
- 656 47. Snijder J, Kononova O, Barbu IM, Utrecht C, Rurup WF, Burnley RJ, Koay MST,
657 Cornelissen JJLM, Roos WH, Barsegov V, Wuite GJL, Heck AJR. 2016. Assembly and
658 mechanical properties of the cargo-free and cargo-loaded bacterial nanocompartment
659 encapsulin. *Biomacromolecules* **17**:2522-2529.
660
- 661 48. Katen S, Zlotnick A. 2009. The thermodynamics of virus capsid assembly. *Methods*
662 *Enzymol* **455**:395-417.
663
- 664 49. Perlmutter JD, Hagan MF. 2015. Mechanism of virus assembly. *Annu Rev Phys Chem*
665 **66**:217-239.
666
- 667 50. Perlmutter JD, Mohajerani F, Hagan MF. 2016. Many-molecule encapsulation by an
668 icosahedral shell. *eLife* **5**:e14078.
669
- 670 51. Huang RK, Khayat R, Lee KK, Gertsman I, Duda RL, Hendrix RW Johnson JE. 2011.

McDowell and Hoiczky **Running title:** Bacterial nanocompartments

- 671 The Prohead-I structure of bacteriophage HK97: implications for scaffold-mediated
672 control of particle assembly and maturation. *J Mol Biol* **408**:541-554.
673
- 674 52. Conway JF, Duda RL, Cheng N, Hendrix RW, Steven AC. 1995. Proteolytic and
675 conformational control of virus capsid maturation: the bacteriophage HK97 system. *J*
676 *Mol Biol* **253**:86-99.
677
- 678 53. Tetter S, Terasaka N, Steinauer A, Bingham RJ, Clark S, Scott AJP, Patel N, Leibundgut
679 M, Wroblewski E, Ban N, Stockley PG, Twarock R, Hilvert D. 2021. Evolution of a
680 virus-like architecture and packaging mechanism in a repurposed bacterial protein.
681 *Science* **372**:1220-1224.
682
- 683 54. Tamura A, Fukutani Y, Takami T, Fujii M, Nakaguchi Y, Murakami Y, Noguchi K,
684 Yohda M, Odaka M. 2015. Packaging guest proteins into the encapsulin
685 nanocompartment from *Rhodococcus erythropolis* N771. *Biotechnol Bioeng* **112**:13-20.
686
- 687 55. Cassidy-Amstutz C, Oltrogge L, Going CC, Lee A, Teng P, Quintanilla D, East-Seletsky
688 A, Williams ER, Savage DF. 2016. Identification of a minimal peptide tag for *in vivo*
689 and *in vitro* loading of encapsulin. *Biochemistry* **55**:3461-3468.
690
- 691 56. He D, Hughes S, Vanden-Hehir S, Georgiev A, Altenbach K, Tarrant E, Mackay CL,
692 Waldron KJ, Clarke DJ, Marles-Wright J. (2016). Structural characterization of
693 encapsulated ferritin provides insight into iron storage in bacterial nanocompartments.

McDowell and Hoiczky **Running title:** Bacterial nanocompartments

694 *eLife* **5**:e18972.

695

696 57. Williams EM, Jung SM, Coffman JL, Lutz S. 2018. Pore engineering for enhanced mass
697 transport in encapsulin nanocompartments. *ACS Synth Biol* **7**:2514-2517.

698

699 58. Ross J, McIver Z, Lambert T, Piergentili C, Gallagher KJ, Bird JE, Cruickshank FL,
700 Zarazúa-Arvizu E, Horsfall LE, Waldron KJ, Wilson MD, Mackay CL, Baslé A, Clarke
701 DJ, Marles-Wright J. 2021. Pore dynamics and asymmetry cargo loading in an
702 encapsulin nanocompartment. doi.org/10.1101/2021.04.15.439977. bioRxiv.

703

704 59. Ahmad M, Roberts JN, Hardiman EM, Singh R, Eltis LD, Bugg TD. 2011. Identification
705 of DypB from *Rhodococcus jostii* RHA1 as a lignin peroxidase. *Biochemistry* **50**:5096-
706 5107.

707

708 60. Adamson L, Tasneem N, Andreas MP, Close W, Szyszka TN, Jenner E, Young R,
709 Cheah LC, Norman A, Sainsbury F, Giessen TW, Lau YH. 2021. Pore structure controls
710 stability and molecular flux in engineered protein cages.
711 doi.org/10.1101/2021.01.27.428512. bioRxiv.

712

713 61. Contreras H, Joens MS, McMath LM, Le VP, Tullius MV, Kimmey JM, Bionghi N,
714 Horwitz MA, Fitzpatrick JA, Goulding CW. 2014. Characterization of a *Mycobacterium*
715 *tuberculosis* nanocompartment and its potential cargo proteins. *J Biol Chem* **289**:18279-
716 18289.

McDowell and Hoiczky **Running title:** Bacterial nanocompartments

717

718 62. Rurup WF, Snijder J, Koay MST, Heck AJR, Cornelissen JJLM. 2014. Self-sorting of
719 foreign proteins in a bacterial nanocompartment. *J Am Chem Soc* **136**:3828-3832.

720

721 63. Giessen TW, Silver PA. 2017a. Engineering carbon fixation with artificial protein
722 organelles. *Curr Opin Biotechnol* **46**:42-50.

723

724 64. Snijder J, van de Waterbeemd M, Damoc E, Denisov E, Grinfeld D, Bennett A,
725 Agbandje-McKenna M, Makarov A, Heck AJR. 2014. Defining the stoichiometry and
726 cargo load of viral and bacterial nanoparticles by Orbitrap mass spectrometry. *J Am*
727 *Chem Soc* **136**:7295-7299.

728

729 65. Chung YJ, Krueger C, Metzgar D, Saier MHJr. 2001. Size comparisons among integral
730 membrane transport protein homologues in bacteria, Archaea, and Eucarya. *J Bacteriol*
731 **183**:1012-1021.

732

733 66. Kim SJ, Shoda M. 1999. Purification and characterization of a novel peroxidase from
734 *Geotrichum candidum* dec1 involved in decolorization of dyes. *Appl Environ Microbiol*
735 **65**:1029-1035.

736

737 67. Cannon GC, English RS, Shively JM. 1991. *In situ* assay of ribulose-1,5-biphosphate
738 carboxylase/oxygenase in *Thiobacillus neapolitanus*. *J Bacteriol* **173**:1565-1568.

739

McDowell and Hoiczky **Running title:** Bacterial nanocompartments

- 740 68. Havemann GD, Bobik TA. 2003. Protein content of polyhedral organelles involved in
741 coenzyme B₁₂-dependent degradation of 1,2-propanediol in *Salmonella enterica* serovar
742 Typhimurium LT2. *J Bacteriol* **185**:5086-5095.
743
- 744 69. Yeates TO, Kerfeld CA, Heinhorst S, Cannon GC, Shively JM. 2008. Protein-based
745 organelles in bacteria: carboxysomes and related microcompartments. *Nat Rev Microbiol*
746 **6**:681-691.
747
- 748 70. Tanaka S, Kerfeld CA, Sawaya MR, Cai F, Heinhorst S, Cannon GC, Yeates TO. 2008.
749 Atomic-level models of the bacterial carboxysomes shell. *Science* **319**:1083-1086.
750
- 751 71. Reddy PV, Puri RV, Khera A, Tyagi AK. 2012. Iron storage proteins are essential for
752 the survival and pathogenesis of *Mycobacterium tuberculosis* in THP-1 macrophages
753 and the guinea pig model of infection. *J Bacteriol* **194**:567-575.
754
- 755 72. Andrews SC. 2010. The ferritin-like superfamily: evolution of the biological iron
756 storeman from a rubrerythrin-like ancestor. *Biochim Biophys Acta – General Subjects*
757 **1800**:691-705.
758
- 759 73. Cornelis P, Wei Q, Andrews SC, Vinckx T. 2011. Iron homeostasis and management of
760 oxidative stress response in bacteria. *Metallomics* **3**:540-549.
761
- 762 74. Khademian M, Imlay JA. 2021. How bacterial evolved to tolerate oxygen. *Trends*

McDowell and Hoiczky **Running title:** Bacterial nanocompartments

763 *Microbiol* **29**:428-440.

764

765 75. Kim D, Choi J, Lee S, Hyun H, Lee K, Cho K. 2019. Mutants defective in the
766 production of encapsulin show tan-phase-locked phenotype in *Myxococcus xanthus*. *J*

767 *Microbiol* **57**:795-802.

768

769 76. Stenkamp RE. 1994. Dioxygen and hemerythrin. *Chem Rev* **94**:715-726.

770

771 77. Li X, Tao J, Hu X, Chan J, Xiao J, Mi K. 2014. A bacterial hemerythrin-like protein
772 MsmHr inhibits the SigF-dependent hydrogen peroxide response in mycobacteria. *Front*

773 *Microbiol* **5**:1-11.

774

775 78. Kendall JJ, Barrero-Tobon AM, Hendrixson DR, Kelly DJ. 2014. Hemerythrins in the
776 microaerophilic bacterium *Campylobacter jejuni* help protect key iron-sulphur cluster
777 enzymes from oxidative damage. *Environ Microbiol* **16**:1105-1121.

778

779 79. Kuypers MMM, Sliemers AO, Lavik G, Schmid M, Jørgensen BB, Kuenen JG,
780 Sinninghe Damsté JS, Strous M, Jetten MS. 2003. Anaerobic ammonium oxidation by
781 anammox bacteria in the Black Sea. *Nature* **422**:608-611.

782

783 80. Kartal B, De Almeida NM, Maalcke WJ, Op denCamp HJM, Jetten MSM, Keltjens JT.

784 2013. How to make a living from anaerobic ammonium oxidation. *FEMS Microbiol Rev*

785 **37**:428-461.

McDowell and Hoiczky **Running title:** Bacterial nanocompartments

786

787 81. Tracey JC, Coronado M, Giessen TW, Lau MCY, Silver PA, Ward BB. 2019. The
788 discovery of twenty-eight new encapsulin sequences, including three in anammox
789 bacteria. *Sci Rep* **9**:1-11.

790

791 82. Xing CY, Fan YC, Chen X, Guo JS, Shen Y, Yan P, Fang F, Chen YP. 2020. A self-
792 assembled nanocompartment in anammox bacteria for resisting intracellular
793 hydroxylamine stress. *Sci Total Environ* **717**:137030.

794

795 83. Kartal B, Maalcke WJ, De Almeida NM, Cirpus I, Gloerich J, Geerts W, Op den Camp
796 HJM, Harhangi HR, Janssen-Megens EM, Francoijs KJ, Stunnenberg HG, Keltjens JT,
797 Jetten MSM, Strous M. 2011. Molecular mechanism of anaerobic ammonium oxidation.
798 *Nature* **479**:127-130.

799

800 84. Gong J, Chen M, Zheng Y, Wang S, Wang Y. 2012. Polymeric micelles drug delivery
801 system in oncology. *J Control Release* **159**:312-323.

802

803 85. Allen TM, Cullis PR. 2013. Liposomal drug delivery systems: from concept to clinical
804 application. *Adv Drug Deliv Rev* **65**:36-48.

805

806 86. Ma Y, Nolte RJM, Cornelissen JJLM. 2012. Virus-based nanocarriers for drug delivery.
807 *Adv Drug Deliv Rev* **64**:811-825.

808

McDowell and Hoiczky **Running title:** Bacterial nanocompartments

- 809 87. Rohovie MJ, Nagasawa M, Swartz JR. 2017. Virus-like particles: next generation
810 nanoparticles for targeted therapeutic delivery. *Bioeng Transl Med* **2**:43-57.
811
- 812 88. Andersen ES, Dong M, Nielsen MM, Jahn K, Subramani R, Mamdouh W, Golas MM,
813 Sander B, Stark H, Oliveira CL, Pedersen JS, Birkedal V, Besenbacher F, Gothelf KV,
814 Kjems J. 2009. Self-assembly of a nanoscale DNA box with a controllable lid. *Nature*
815 **459**:73-76.
816
- 817 89. Kumar G, Sinha S. 2021. Biophysical approaches to understand and re-purpose bacterial
818 microcompartments. *Curr Opin Microbiol* **63**:43-51.
819
- 820 90. Lee EJ, Lee NK, Kim IS. 2016. Bioengineered protein-based nanocage for drug
821 delivery. *Adv Drug Deliv Rev* **106**:157-171.
822
- 823 91. Rurup WF, Snijder J, Koay MST, Heck AJR, Cornelissen JJLM. 2014. Self-sorting of
824 foreign proteins in a bacterial nanocompartment. *J Am Chem Soc* **136**:3828-3832.
825
- 826 92. Künzle M, Mangler J, Lach M, Beck T. 2018. Peptide-directed encapsulation of
827 inorganic nanoparticles into protein container. *Nanoscale* **10**:22917-22926.
828
- 829 93. Altenburg WJ, Rollins N, Silver PA, Giessen TW. 2021. Exploring targeting peptide-
830 shell interactions in encapsulin nanocompartments. *Sci Rep* **11**:4951.
831

McDowell and Hoiczky **Running title:** Bacterial nanocompartments

- 832 94. Klem R, de Ruiter MV, Cornelissen JJLM. 2018. Protecting encapsulin nanoparticles
833 with cysteine-knot miniproteins. *Mol Pharm* **15**:2991-2996.
834
- 835 95. Hagen A, Sutter M, Sloan N, Kerfeld CA. 2018 Programmed loading and rapid
836 purification of engineered bacterial microcompartment shells. *Nat Commun* **9**:2881.
837
- 838 96. Jones JA, Cristie-David AS, Andreas MP, Giessen TW. 2021. Triggered reversible
839 disassembly of an engineered protein nanocage. doi.org/10.1101/2021.04.19.440480.
840 bioRxiv.
841
- 842 97. Kennedy NW, Mills CE, Nichols TM, Abrahamson CH, Tullman-Ercek D. 2021.
843 Bacterial microcompartments: tiny organelles with big potential. *Curr Opin Microbiol*
844 **63**:36-42.
845
- 846 98. Lau YH, Giessen TW, Altenburg WJ, Silver PA. 2018. Prokaryotic nanocompartments
847 form synthetic organelles in a eukaryote. *Nat Commun* **9**:1311.
848
- 849 99. Sigmund F, Massner C, Erdmann P, Stelzl A, Rolbieski H, Desai M, Bricault S, Wörner
850 TP, Snijder J, Geerlof A, Fuchs H, Hrabe de Angelis M, Heck AJR, Jasanoff A,
851 Ntziachristos V, Plitzko J, Westmeyer GG. 2018. Bacterial encapsulins as orthogonal
852 compartments for mammalian cell engineering. *Nat Commun* **9**:1990.
853
- 854 100. Sigmund F, Pettinger S, Kube M, Schneider F, Schifferer M, Schneider S, Efremova

McDowell and Hoiczky **Running title:** Bacterial nanocompartments

- 855 MV, Pujol-Martí J, Aichler M, Walch A, Misgeld T, Dietz H, Westmeyer GG. 2019.
856 Iron-sequestering nanocompartments as multiplexed electron microscopy gene reporters.
857 *ACS Nano* **13**:8114-8123.
858
- 859 101. Tatsis N, Ertl HCJ. 2004. Adenoviruses as vaccine vectors. *Mol Ther* **10**:616-629.
860
- 861 102. Hasanpourghadi M, Novikov M, Ertl HCJ. 2021. Covid-19 vaccines based on
862 adenovirus vectors. *Trends Biochem Sci* **46**:429-430.
863
- 864 103. Fiers W, De Filette M, Birkett A, Neiryneck S, Min Jou W. 2004. A “universal”
865 human influenza A vaccine. *Virus Res* **103**:173-176.
866
- 867 104. Lagoutte P, Mignon C, Stadthagen G, Potisopon S, Donnat S, Mast J, Lugari A,
868 Werle B. 2018. Simultaneous surface display and cargo loading of encapsulin
869 nanocompartments and their use for rationale vaccine design. *Vaccine* **36**:3622-3628.
870
- 871 105. Choi B, Moon H, Hong SJ, Shin C, Do Y, Ryu S, Kang S. 2016. Effective delivery
872 of antigen-encapsulin nanoparticle fusions to dendritic cells leads to antigen-specific
873 cytotoxic T cell activation and tumor rejection. *ACS Nano* **10**:7339-7350.
874
- 875 106. Brigger I, Dubernet C, Couvreur P. 2012. Nanoparticles in cancer therapy and
876 diagnosis. *Adv Drug Deliv Rev* **64**:24-36.
877

McDowell and Hoiczky **Running title:** Bacterial nanocompartments

- 878 107. Gabashvili AN, Chmelyuk NS, Efremova MV, Malinovskaya JA, Semkina AS,
879 Abakumov MA. 2020. Encapsulins – bacterial protein nanocompartments: structure,
880 properties, and application. *Biomolecules* **10**:966.
- 881
- 882 108. Toita R, Murata M, Abe K, Narahara S, Piao JS, Kang JH, Hashizume M. 2013. A
883 nanocarrier based on a genetically engineered protein cage to deliver doxorubicin to
884 human hepatocellular carcinoma cells. *Chem Commun* **49**:7442-7444.
- 885
- 886 109. Moon H, Lee J, Kim H, Heo S, Min J, Kang S. 2014. Genetically engineering
887 encapsulin protein cage nanoparticle as a SCC-7 cell targeting optical nanoprobe.
888 *Biomater Res* **18**:21.
- 889
- 890 110. Putri RM, Allende-Ballester C, Luque D, Klem R, Rousou K-A, Liu A, Traulsen
891 CH-H, Rurup WF, Koay MST, Castón JR, Cornelissen JJLM. 2017. Structural
892 characterization of native and modified encapsulins as nanoplatfoms for *in vitro*
893 catalysis and cellular uptake. *ACS Nano* **11**:12796-12804.
- 894
- 895 111. Sonotaki S, Takami T, Noguchi K, Odaka M, Yohda M, Murakami Y. 2017.
896 Successful PEGylation of hollow encapsulin nanoparticles from *Rhodococcus*
897 *erythropolis* N771 without affecting their disassembly and reassembly properties.
898 *Biomater Sci* **5**:1082-1089.
- 899
- 900 112. Minten IJ, Claessen VI, Blank K, Rowan AE, Nolte RJM, Cornelissen JJLM. 2011.

McDowell and Hoiczky **Running title:** Bacterial nanocompartments

- 901 Catalytic capsids: the art of confinement. *Chem Sci* **2**:358-362.
- 902
- 903 113. Giessen TW, Silver PA. 2016. Converting a natural protein compartment into a
904 nanofactory for the size-constrained synthesis of antimicrobial silver particles. *ACS*
905 *Synth Biol* **5**:1497-1504.
- 906
- 907 114. Lee TH, Carpenter TS, D'haeseleer, P, Savage DF, Yung MC. 2020. Encapsulin
908 carrier proteins for enhanced expression of antimicrobial peptides. *Biotechnol Bioeng*
909 **117**:603-613.
- 910
- 911 115. Jenkins MC, Lutz S. 2021. Encapsulin nanocontainers as versatile scaffolds for the
912 development of artificial metabolons. *ACS Synth Biol* **10**:857-869.
- 913
- 914 116. Putri RM, Fredy JW, Cornelissen JJLM, Koay MST, Katsonis N. 2016. Labelling
915 bacterial nanocages with photo-switchable fluorophores. *ChemPhysChem* **17**:1815-1818.
- 916
- 917 117. Wan W, Zhu MQ, Tian Z, Li ADQ. 2015. Antiphase dual-color correlation in a
918 reactant – product pair imparts ultrasensitivity in reaction-linked double-photoswitching
919 fluorescence imaging. *J Am Chem Soc* **137**:4312-4315.
- 920
- 921 118. Bae Y, Kim GJ, Kim H, Park SG, Jung HS, Kang S. 2018. Engineering tunable dual
922 functional protein cage nanoparticle using bacterial superglue. *Biomacromolecules*
923 **19**:2896-2904.

McDowell and Hoiczky **Running title:** Bacterial nanocompartments

924

925 119. Zeth K, Hoiczky E, Okuda M. 2016. Ferroxidase-mediated iron oxide
926 biomineralization: novel pathways to multifunctional nanoparticles. *Trends Biochem Sci*
927 **41**:190-203.

928

929 120. Zhang Y, Wang X, Chu C, Zhou Z, Chen B, Pang X, Lin G, Lin H, Guo Y, Ren E,
930 Lv P, Shi Y, Zheng Q, Yan X, Chen X, Liu G. 2020. Genetically engineered magnetic
931 nanocages for cancer magneto-catalytic therapy. *Nat Commun* **11**:5421.

932

McDowell and Hoiczky **Running title:** Bacterial nanocompartments

933 **Figure legends:**

934

935 **FIG 1** Structures of selected bacterial proteinaceous compartments inside and outside of the
936 context of a bacterial cell. All structures within each context are drawn to scale to provide a
937 perspective of their relative size in a cell as well as to each other. On the right, atomic level
938 models of (A) the polyhedral shell of the CO₂-fixing carboxysome from *Synechocystis*
939 PCC6803 (T=75, 120 nm), the atomic structures of the iron-sequestering encapsulin shells of
940 (B) *Q. thermotolerans* (T=4, 48 nm, PDB 6NJ8), (C) *M. xanthus* (T=3, 32 nm, PDB 4PT2)
941 and (D) *T. maritima* (T=1, 24 nm, PDB 3DKT); the crystal structure of (E) ferritin from
942 *Rhodobacter sphaeroides* (12 nm, PDB 3GVY) and the structure of (F) the proteasome from
943 *M. tuberculosis* (15x11.5 nm, PDB 3MI0). Note, that for the long buoyancy-providing
944 spindle-shaped gas vesicle on the left currently no atomic model exists and it was therefore
945 omitted from the atomic structures. The carboxysome structure is reproduced from reference
946 [70](#) with permission of the publisher.

947

948

949 **FIG 2** Schematic overview of various strategies for using encapsulin systems in bio-
950 nanotechnology. The four sections of the prototype encapsulin show how the interior,
951 surface and structure of the encapsulin shell can be modified to functionalize the particle. *In*
952 *vivo* packaging takes advantage of the fact that any heterologous CLP-tag-carrying protein
953 will be packaged as cargo (various colored shapes) that then can i.e. precipitate metals like
954 iron (red small circle). Surface labeling relies on the fact that each shell monomer can be
955 either chemically coupled *via* a linker to small molecules or proteins (green spheres, purple

McDowell and Hoiczky **Running title:** Bacterial nanocompartments

956 squares and yellow hexamers) or modified through the genetic-based incorporation of a
957 peptide sequence into the shell protein itself (brown rods and blue triangles). Shell design
958 aims at modifying properties of the encapsulin shell by changing the size, charge or gating of
959 the shell pores as well as other physical parameters of the structure. Finally, *in vitro*
960 packaging takes advantage of the ability of encapsulins to repeatedly disassemble and
961 reassemble. During the reassembly, any externally present inorganic structure such as a
962 metal particle (large red sphere), protein (pink pentamer) or small molecule (variable shapes)
963 will be packaged as long as they allow the formation of the closed shell to occur. Recently
964 achieved fine tuning of the disassembly and reassembly process may allow packaging under
965 physiological conditions. Importantly, these cargos do not necessarily need to have a CLP.

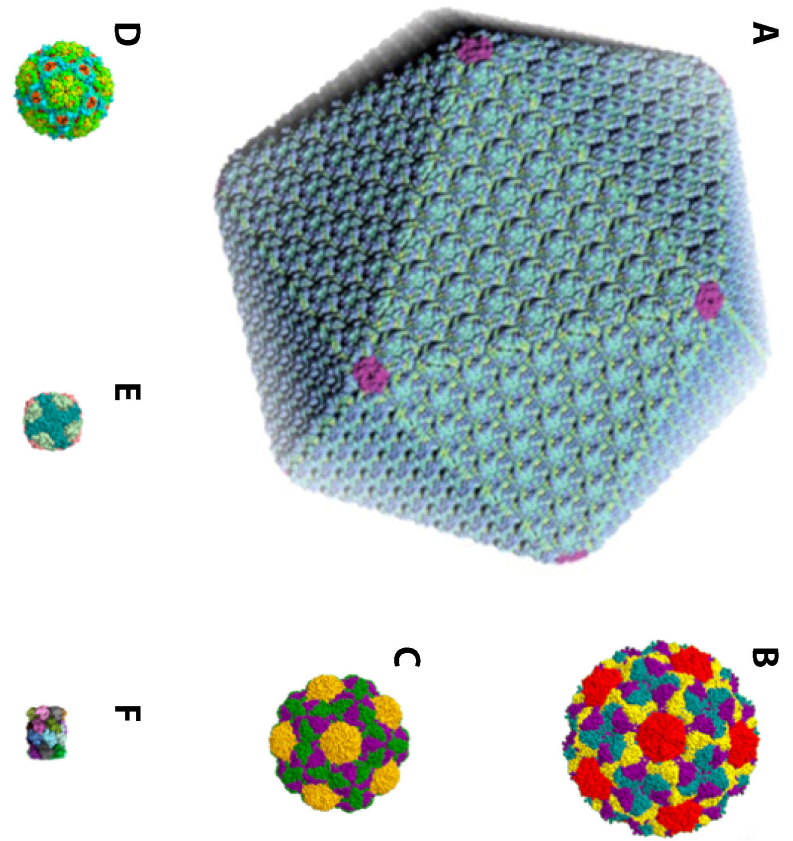
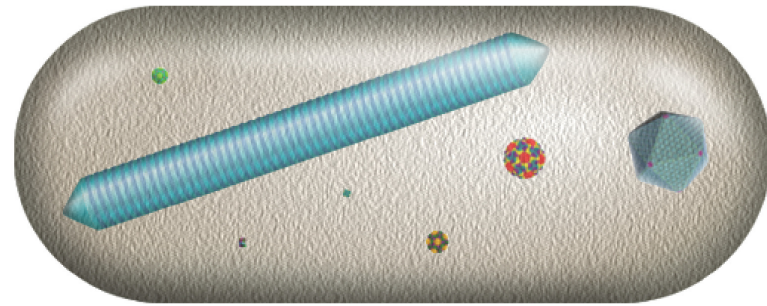
966

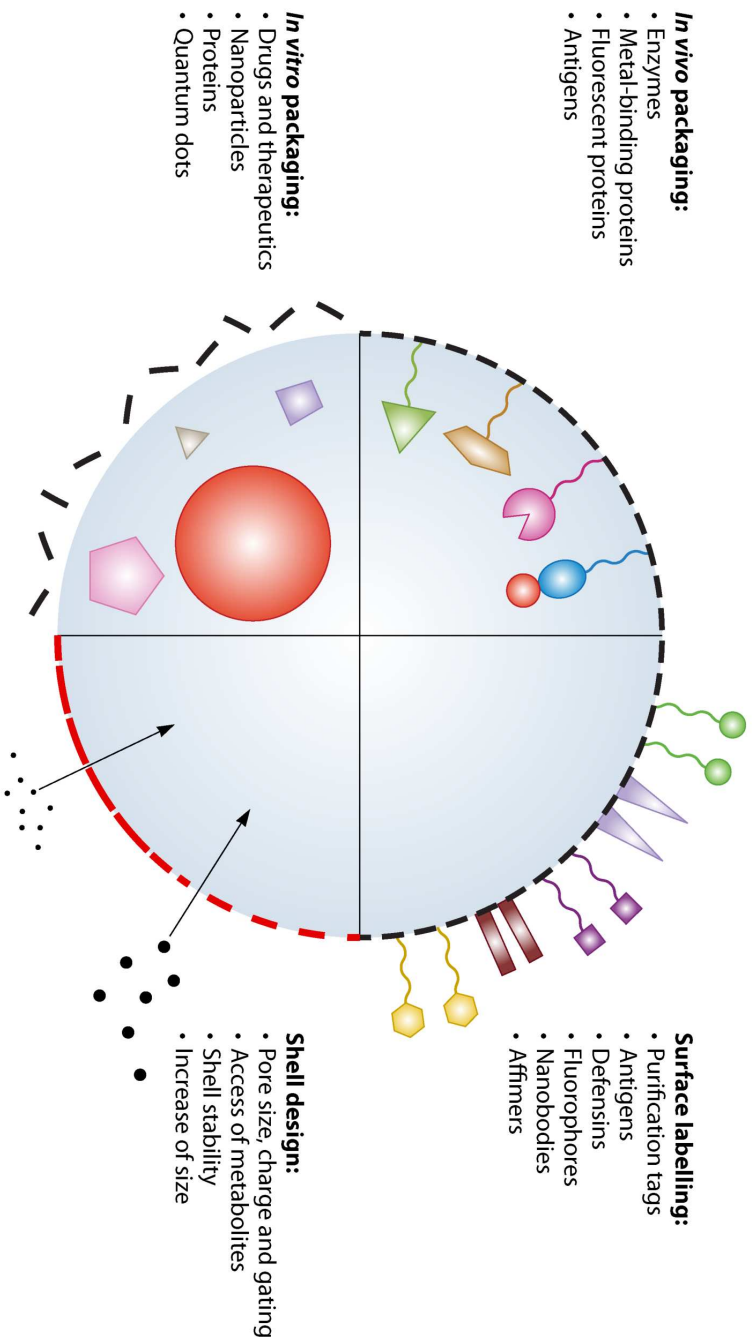
967

968 **Table legends:**

969

970 **Table 1** Structural characteristics for a representative selection of bacterial nano- and
971 microcompartments. For the nanocompartments examples have been included containing
972 shell proteins with (encapsulins) or without the HK97-fold (non-encapsulins). The
973 assignment of encapsulin families is based on recently published data (28). When known, the
974 corresponding T-values are listed. Of note, the only difference between nano- and
975 microcompartments is their size – structures with a diameter smaller than 100 nm are
976 classified as nanocompartments those larger than 100 nm as microcompartments.





	T-value	Monomers per shell	Diameter (nm)	Cargo	Encapsulin Family	Reference
Nanocompartments (size < 100 nm)						
Encapsulins						
<i>Q. thermotolerans</i> encapsulin	4	240	42	Ferritin-like protein	1	22
<i>M. xanthus</i> encapsulin	3	180	32	Ferritin-like protein	1	17
<i>P. furiosus</i> encapsulin	3	180	32	Ferritin-like protein	1	24
<i>T. maritima</i> encapsulin	1	60	24	Ferritin-like protein	1	15
<i>M. smegmatis</i> encapsulin	1	60	24	Dye- decolourising peroxidase	1	20
<i>S. elongatus</i> encapsulin	1	60	24.5	Cysteine desulfurase	2a	23
Non-encapsulins						
HK97 phage capsid	7	420	66	Double stranded DNA	-	30
<i>Bacillus subtilis</i> lumazine synthase	1	60	16	Riboflavin synthase	-	31
Microcompartments (size > 100 nm)						
Gas vesicles	-	-	45 – 120 Length - 100 – 1400	Gases	-	7, 32
α - Carboxysome	75	4500	120	Ribulose-1,5-bisphosphate carboxylase/oxygenase and carbonic anhydrase	-	70
β - Carboxysome	-	-	200-400	Ribulose-1,5-bisphosphate carboxylase/oxygenase and carbonic anhydrase	-	33
Pdu Compartment	-	-	80 – 120	Vitamin B 12-dependent propanediol dehydratase	-	34

Table 1